VIRTUALLY ROTATED MEMS GYROSCOPE WITH ANGLE OUTPUT

Igor P. Prikhodko, Jeffrey A. Gregory, and Michael W. Judy
Analog Devices Inc., Wilmington, Massachusetts, USA

ABSTRACT

We experimentally demonstrate a virtually rotated MEMS Rate Integrating Gyroscope (RIG) with 0.0015 °/√Hz angle white noise, 0.0085° angle flicker, and 0.02 °/s/√Hz angle random walk. RIGs exhibit unlimited full scale range and bandwidth, but frequency/damping mismatch imperfection arising from fabrication set a rate threshold below which the RIGs fail to operate. Here we show that by applying virtual rotation using the gyroscope's control electrodes along with dynamic mismatch controls, the angle-dependent bias drifts are averaged out, allowing measurement of rotation rates lower than 0.1 °/s, which is two orders of magnitude below the rate threshold value. The presented methods may enable commercialization of angle measuring MEMS gyroscopes.

INTRODUCTION

RIGs are thought to be impractical in MEMS due to the manufacturing tolerances required to compete with conventional micromachined rate gyroscopes, which are generally less susceptible to fabrication imperfections. The limitation of the majority of published RIGs [1-3] is an inability to measure input rates below a certain threshold. Demonstration of angle operation [1-3] is often performed at input rates above 50 °/s due to damping and stiffness mismatches. The methods in [2,3] relying on continuous identification and cancellation of the damping mismatch require complex controls. In this work we apply a virtual rate (self-precession) significantly larger than the damping mismatch and experimentally demonstrate that the angle drift reduces linearly with the virtual rate according to the theory and simulations presented previously in [4]. In practice the maximum virtual rate that can be applied to the RIG is, however, bounded by the available force authority, so here we combine the virtual rotation with the dynamic mismatch control from [2] and experimentally demonstrate measurement of the rotation rates below the threshold value.

THEORY

Rate Integrating Gyroscope Background

We summarize and extend our theory presented in [4] to include effects of the frequency mismatch. In presence of damping $\Delta(1/\tau) = 1/\tau_x - 1/\tau_y$ and frequency $\Delta\omega = \omega_x - \omega_y$ mismatches the precession angle θ dynamic is given by [5]:

$$\dot{\theta} = -\Omega + \frac{1}{2}\Delta\left(\frac{1}{\tau}\right)\sin 2(\theta - \theta_\tau) + \frac{\Delta\omega}{2}\cos 2(\theta - \theta_\omega)\frac{Q}{E}, \quad (1)$$

where τ_x, τ_y are the damping time constants, ω_x, ω_y are the natural frequencies, θ_τ, θ_ω are the principal axes of damping and stiffness, E,Q are the energy and quadrature variables, $\Omega = \kappa\Omega_{true} + V_{virt}/(2\omega\sqrt{E})$ is a sum of the true input rate with angular gain κ and the virtual rate defined by the force corresponding to a voltage command V_{virt}. In [4] we focused on damping mismatch and ignored the frequency mismatch effects by assuming that quadrature is nulled by a PID loop.

Fig. 1: Photo of a packaged MEMS gyroscope (4×6×1 mm²) used as a test vehicle for virtual rotation demonstration.

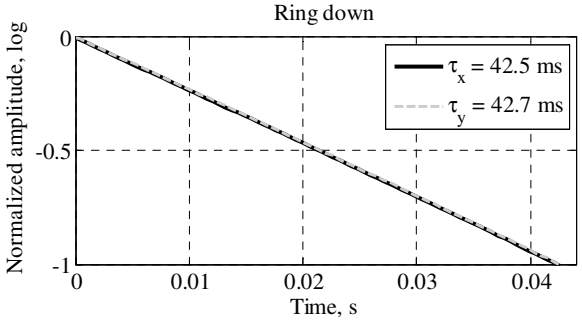

Fig. 2: Measured ring-down revealing damping mismatch $\Delta(1/\tau) = 1/\tau_x - 1/\tau_y$ = 6 %s, which defines RIG rate threshold.

In reality, however, a non-zero Q loop residual makes it impossible to ignore effects of the frequency mismatch (due to offsets in electronics and other errors; this is the case even when integral gain is used). Assuming E, Q are constants, the Eqn. (1) can be simplified to:

$$\dot{\theta} = -\Omega + \Omega_{th}\sin 2(\theta - \theta_{lock}), \quad (2)$$

where the threshold rate Ω_{th} and the angle θ_{lock} are given by:

$$\Omega_{th}^2 = \frac{1}{4}\Delta\left(\frac{1}{\tau}\right)^2 + \left(\frac{\Delta\omega Q}{2E}\right)^2 - \Delta\left(\frac{1}{\tau}\right)\frac{\Delta\omega Q}{2E}\sin 2(\theta_\tau - \theta_\omega), \quad (3)$$

$$\tan 2\theta_{lock} = \frac{\Delta(1/\tau)\sin 2\theta_\tau - \Delta\omega\cos 2\theta_\omega(Q/E)}{\Delta(1/\tau)\cos 2\theta_\tau + \Delta\omega\sin 2\theta_\omega(Q/E)}. \quad (4)$$

The form of Eqn. (2) is exactly what we solved in [4]. The solution depends on whether $|\Omega_{th}|$ is greater or less than $|\Omega|$. The closed-form solution for the case $|\Omega|<|\Omega_{th}|$ is given by:

$$\theta \approx \theta_{lock} + \begin{cases} \pi/2 - \Omega/(2\Omega_{th}) + \pi k : \Omega_{th} > 0 \\ \Omega/(2\Omega_{th}) + \pi k : \Omega_{th} < 0 \end{cases}, k \in \mathbb{Z}, \quad (5)$$

revealing that the precession angle converges to a constant angle which is a function of rate, effectively forcing a sensor to act as a rate rather than a rate integrating gyroscope. The closed-form solution for the case $|\Omega|>|\Omega_{th}|$ is given by:

$$\theta \approx \theta_{lock} - \kappa_{eff}\Omega t + (\Omega_{th}/2\Omega)\left(1 + \cos 2\left(\kappa_{eff}\Omega t + C\right)\right) - C, \quad (6)$$

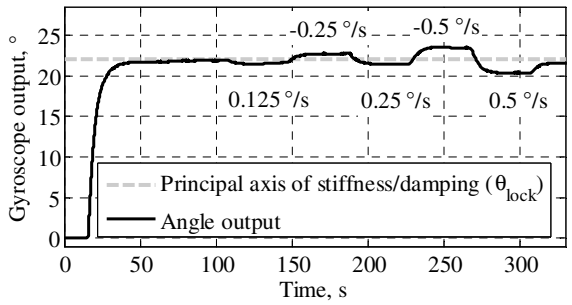

Fig. 3: Measured RIG output shows inability to perform angle measurements for rotations below the rate threshold.

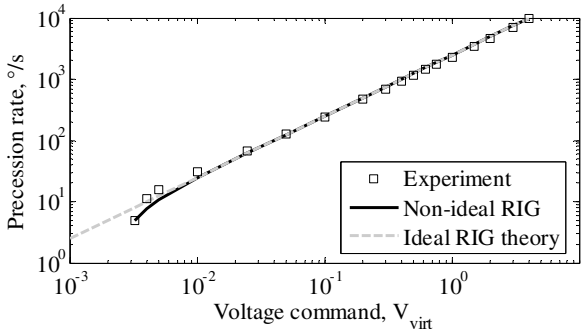

Fig. 4: Measured virtual rate as a function of voltage V_{virt}.

where $\kappa_{\text{eff}} = (1 - (\Omega_{\text{th}}/\Omega)^2)^{1/2} \approx 1 - (\Omega_{\text{th}}/\Omega)^2/2$ is an effective angular gain and C is the integration constant. The Eqn. (6) reveals that the damping and stiffness anisotropy Ω_{th} reduce angular gain from an ideal value of 1, or equivalently leads to angle drift of $\Omega^2_{\text{th}}/(2\Omega)$. A non-ideal RIG output also contains a periodic function of an amplitude $\Omega_{\text{th}}/(2\Omega)$ and a frequency $2\kappa_{\text{eff}}\Omega$, which is often referred to as 2nd harmonic.

Overcoming Rate Threshold by Virtual Rotation

The adverse effects of damping and stiffness anisotropy can be mitigated by applying higher rates of rotation. As evident from Eqn. (6) as rate increases the angular gain converges to its true value of 1 and also the amplitude of the second harmonic reduces linearly. The same effect can be accomplished by using control electrodes to create a virtual rate much greater than the rate threshold value, $|\Omega_{\text{virt}}| = |V_{\text{virt}}/(2\omega\sqrt{E})| > |\Omega_{\text{th}}|$. The forces for applying virtual rate are the same as the ones used to operate the gyroscope in a force-to-rebalance mode [5]. The true input angle $\int\Omega_{\text{true}}$ is then obtained by removing the virtual angle $\theta/\kappa - \Omega_{\text{virt}}t$ from the output. Virtual rate effectively modulates all of the d.c. errors up to the virtual rotation rate (in Hz) and averages out damping and stiffness errors during each rotation period:

$$\int_0^{\pi}(\dot{\theta}+\Omega) = \frac{1}{2}\Delta\left(\frac{1}{\tau}\right)\int_0^{\pi}\sin 2(\theta-\theta_{\tau}) + \frac{\Delta\omega Q}{2E}\int_0^{\pi}\cos 2(\theta-\theta_{\omega}) = 0 \cdot$$

Dynamic Mismatch Controls for Angle Drift Reduction

The dynamic mismatch controls described in [2] are an expansion of the work by Zhbanov [6]. The controls use a 2θ model of the damping and stiffness anisotropy [5], and reduces variations of the energy E_{PID} and quadrature Q_{PID} controls as functions of the gyroscope precession angle θ by applying the following control forces:

$$E_{\text{PID}} = A_{PE}(E - E_0),\ Q_{\text{PID}} = A_{PQ}Q, \tag{7}$$

$$\begin{bmatrix}\Delta D \\ D_{xy}\end{bmatrix} = \sum A_{IE}(E-E_0)\dot{\theta}\begin{bmatrix}\sin 2\theta \\ \cos 2\theta\end{bmatrix}, \tag{8}$$

$$\begin{bmatrix}\Delta K \\ K_{xy}\end{bmatrix} = \sum A_{IK}Q\begin{bmatrix}\sin 2\theta \\ -\cos 2\theta\end{bmatrix}, \tag{9}$$

where A_{PE}, A_{PQ} are proportional and A_{IE}, A_{IK} are integral gains chosen for the stable RIG operation. The identified terms $\Delta D = D_{xx} - D_{yy}$, D_{xy}, $\Delta K = K_{xx} - K_{yy}$, K_{xy} correspond, with proper scaling, to the physical terms of damping and stiffness anisotropy when the principal axes of damping and stiffness align with the reference axes (x,y) of the RIG. These terms are added to output forces to compensate for angle-dependent bias drift and frequency variations as in [2].

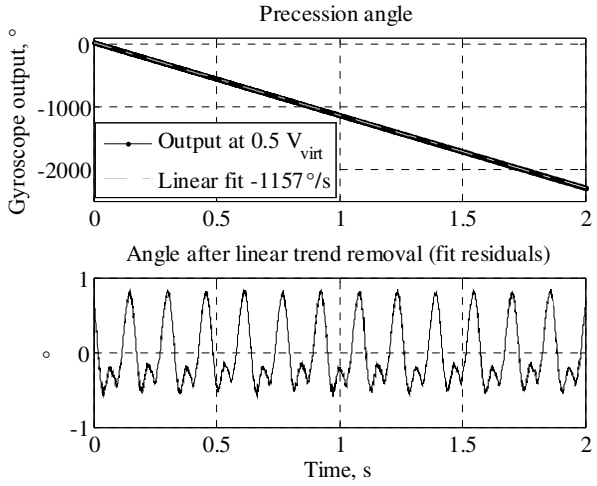

Fig. 5: Time history of the RIG angle output at V_{virt} = 0.5 V.

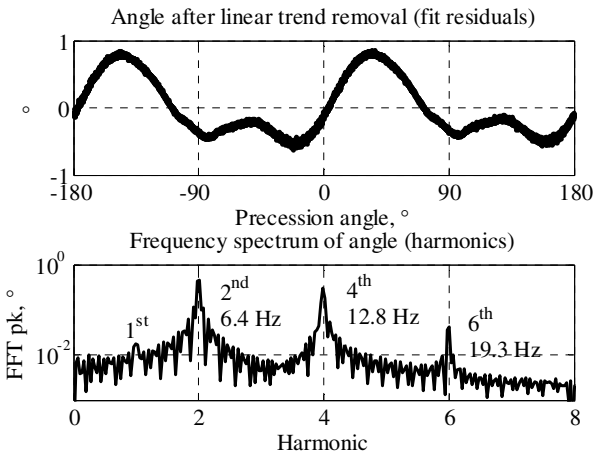

Fig. 6: Precession angle from Fig. 5 after virtual rate removal and its frequency spectrum showing 2nd and 4th harmonics.

EXPERIMENTAL RESULTS

The whole angle, virtual rotation and dynamic mismatch controls were implemented using the real-time toolkit of the Zurich Instruments HF2LI. A photograph of a packaged

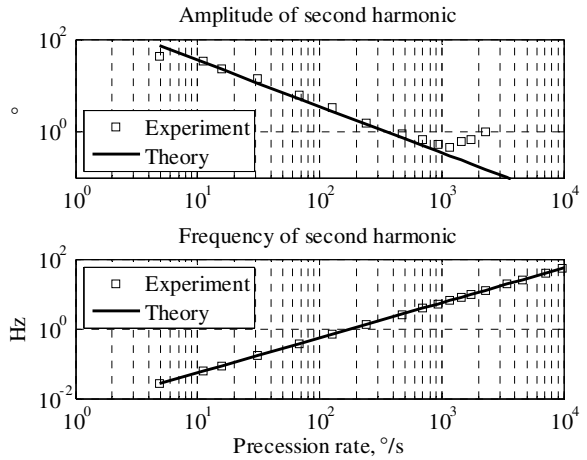

Fig. 7: Reduction of 2nd harmonic amplitude with virtual rate.

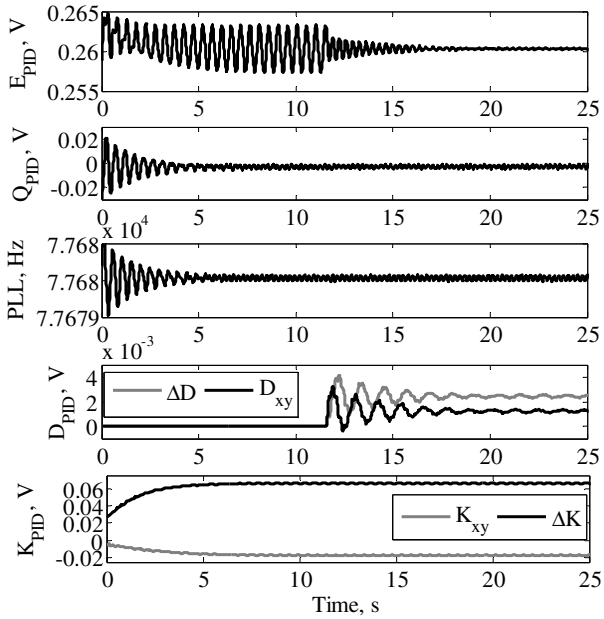

Fig. 8: Measured convergence of dynamic mismatch control (D,K) reducing variations of RIG control loops (Q,E,PLL).

MEMS gyroscope used as a test vehicle is shown in Fig. 1. The damping mismatch was measured by ring-down tests revealing $\Delta(1/\tau) = 1/\tau_x - 1/\tau_y = 6$ °/s, which, in turn defined RIG rate threshold, Fig. 2. Experimentally measured RIG output for the case $|\Omega|<|\Omega_{th}| = \Delta(1/\tau)/(2\kappa) = 6$ °/s assuming $\kappa = 0.5$ and negligible frequency mismatch is shown in Fig. 3. For zero input rate the gyroscope stayed at the angle θ_{lock} = 22° defined by the principal axes of stiffness and damping, see Eqn. (4). As expected from theory, for each applied rate ±0.1, 0.25, 0.5 °/s the sensor's output converged to a steady-state angle value effectively demonstrating behavior of a rate measuring sensor rather than a rate integrating gyroscope.

In order to overcome rate threshold and enable angle measurements virtual rotation $|\Omega|>|\Omega_{th}|$ was applied. Fig. 4 shows an experimentally measured virtual rate as a function of applied voltage, V_{virt} demonstrating self-precession rates as low as 6 °/s (3 mV) and as high as 10,000 °/s (~4 V). The

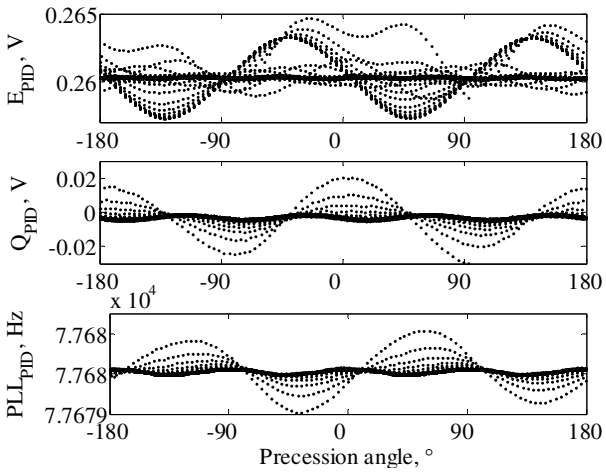

Fig. 9: Fig. 8 data plotted against angle instead of time.

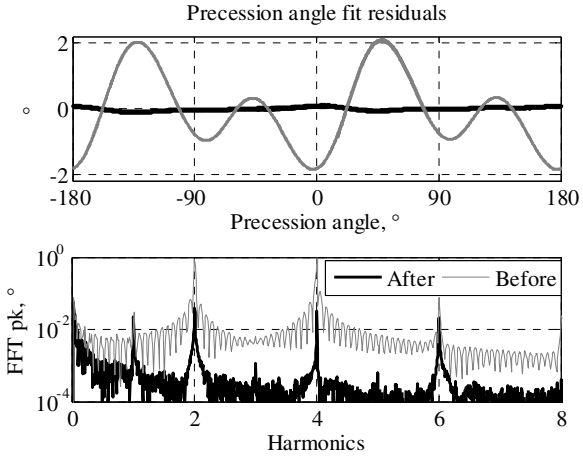

Fig. 10: Measured output with virtual rate removed showing angle error before and after dynamic mismatch control.

experimental data was fitted to a theory using Eqn. (6) showing that as the rotation rate increases the precession rate of a non-ideal RIG $\kappa_{eff}\Omega$ approaches the ideal value $\kappa\Omega$ because damping and stiffness mismatch errors average faster, demonstrating why RIG excel at measuring high rates.

The RIG angle output at V_{virt} = 0.5 V is shown in Fig. 5. A linear fit to the data revealed the self-precession rate of –1157 °/s. In order to measure angle errors the linear trend was removed and fit residuals were analyzed. As expected from Eqn. (6), the angle residuals were periodic as evident from the time domain Fig. 5. Plotting the angle residuals versus precession angle made it possible to recognize both the $\sin 2\theta$ and $\sin 4\theta$ patterns, Fig. 6. A fast Fourier transform was applied and revealed amplitudes of 0.5° and 0.3° for the 2nd and 4th harmonics, respectively. The primary advantage of virtual rotation is that it reduces the magnitude of the harmonics linearly with applied virtual rate, as evident from Fig. 7 where the amplitude of 2nd harmonic was reduced from 50° to 0.5°. Although 2nd harmonic was primarily characterized, virtual rotation also reduces higher order terms. A virtual rate increase beyond 10^3 °/s did not further reduce the amplitude of harmonics, likely due to additional

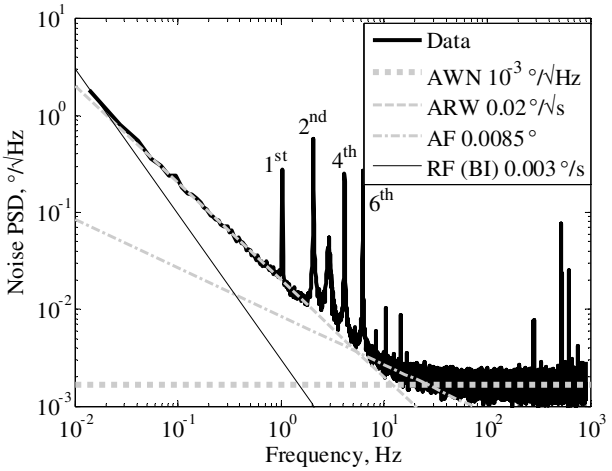

Fig. 11: Noise PSD of a virtually rotated RIG angle output.

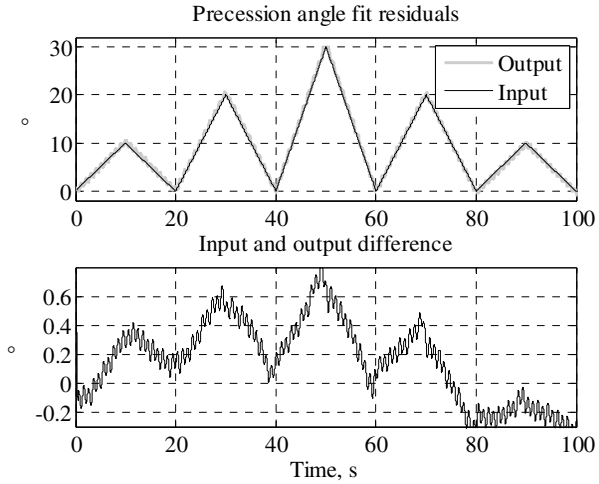

Fig. 12: Measured RIG response to ±1, ±2.5, ±4 °/s *input rates after virtual angle removal showing below* 1° *error.*

drifts introduced by traditional whole-angle control loops lagging the current precession angle in a rapidly rotating gyroscope resulting in a large residual quadrature.

Further improvement was possible by employing the dynamic mismatch control which complement virtual rotation method of drift reduction since it works best when the RIG is rotating. Fig. 8 shows the effect of these control loops on energy, quadrature and frequency control variation on the RIG output with ~300 °/s virtual rotation. A stiffness mismatch control is enabled at time 0 and a damping mismatch control is enabled around 12 s. The ΔK and K_{xy} terms reduce the fluctuation in the quadrature and frequency controls loops by adding frequency tuning and cross-axis stiffness forces. Damping controls ΔD and D_{xy} reduces the variation of the energy loop and reduces drift due to cross-axis damping. Plotting the control functions against angle instead of time (Fig. 9) shows how as the controls converge the 2θ terms in E_{PID}, Q_{PID} and PLL_{PID} are reduced until there is almost no angle dependency. These improvements lead to reduction of angle dependent drift reducing amplitudes of both 2nd, 4th, and 6th harmonics to below 0.03°, Fig. 10.

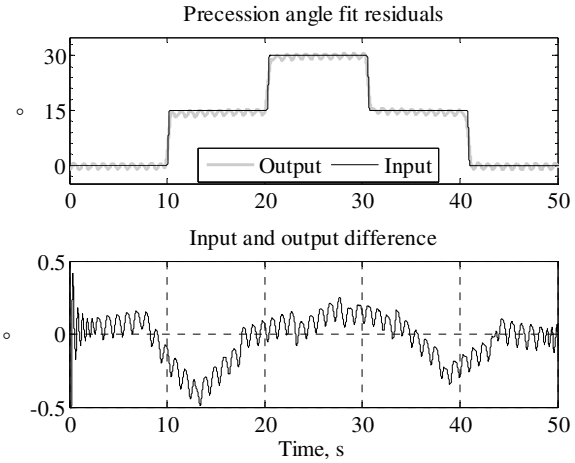

Fig. 13: The RIG response to ±15° *turntable angle change.*

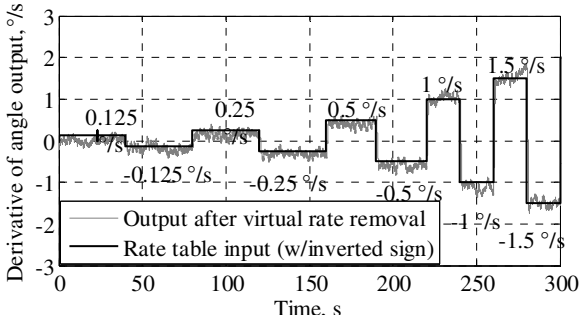

Fig. 14: Demonstration of rate measurement as low as 0.1 °/s.

CONCLUSIONS

The power spectrum of the angle output recorded for 1,500 s (after virtual rate removal) revealed 0.0015 °/√Hz angle white noise, 0.0085° angle flicker, 0.02 °/s/√Hz angle random walk, and 11 °/hr bias instability, Fig. 11. With these settings we performed series of experiments using a rate table showing ability of a RIG to measure rates lower than 0.1 °/s, orders of magnitude below the rate threshold, Figs. 12-14.

ACKNOWLEDGEMENTS

Authors would like to thank Dr. Bugrov from Moscow State University, Russia for help with RIG theoretical model.

REFERENCES

[1] I.P. Prikhodko, et al., *Sensors and Actuators A: Physical*, vol. 177, pp. 67-78, April 2012.

[2] J.A. Gregory et al., *Proc. of IEEE/ION Position Location and Navigation Symposium 2012*, pp. 252-258.

[3] P. Taheri-Tehrani et al., *Proc. IEEE International Symposium on Inertial Sensors and Systems'16,* pp. 9-12.

[4] I. Prikhodko et al., *Proc. IEEE International Symposium on Inertial Sensors and Systems 2016,* pp. 5-8.

[5] D. Lynch, Proc. *2nd St. Petersburg Conf. on Gyroscopic Technology and Navigation*, 1995, pp. 26-34.

[6] Yu. K Zhbanov, *Mechanics of Solids*, vol. 43, no. 3, pp. 328-332, 2008.